

SUSY Search in TeV Scale Polarized Photon-Proton Collisions

Z.Z.Aydin, A. Kandemir, O.Yılmaz and A.U. Yilmazer

Ankara University, Faculty of Sciences

Department of Engineering Physics

06100 Tandoğan, Ankara - Turkey

Production of supersymmetric particles in TeV scale polarized photon-proton collisions is discussed. Polarizations of both photon and proton beams are considered. Associated productions of squark-chargino and squark-gluino, and production of squark pairs have been examined. Although the cross sections for different initial beam polarizations do not differ much, the polarization asymmetry is sensitive to the sparticle mass. We conclude that the capacity of future linac-ring type TeV scale photon-proton colliders is quite promising in the search for SUSY particles.

I. INTRODUCTION

In recent years in addition to the well known TeV scale colliders such as $pp(p\bar{p})$, ep and e^+e^- machines the possibilities of the realization of γe , $\gamma\gamma$ and γp colliders have been proposed and discussed in detail [1]. Here one of the main motivations is to reach the TeV scale at a subprocess level. The collisions of protons from a large hadron machine with electrons from a linac is the most efficient way of achieving TeV scale at a constituent level in ep collisions [2]. A further interesting feature is the possibility of constructing γp colliders on the base of linac-ring ep -machines. This can be realized by using the beam of high energy photons produced by the Compton backscattering of laser photons off a beam of linac electrons. Actually this method was originally proposed to construct γe and $\gamma\gamma$ colliders on the bases of e^+e^- linacs [Ginzburg et.al ref.1]. For the physics program at γe and $\gamma\gamma$ machines see Refs. [3,4]. Recently different physics phenomena which can be investigated at γp colliders have been considered in a number of papers [5–7]. It seems that these machines may open new possibilities for the investigations of the Standard Model and beyond it. For a review see Ref. [8].

On the other hand, among the various extensions beyond the SM the supersymmetry idea seems to be a well-motivated strong candidate to investigate the new physics around TeV scale [10]. In SUSY inspired models the usual particle spectrum is doubled at least; every particle has a superpartner differing in spin by a half unit. Also two Higgs doublets are needed to give mass to both up and down quarks and make the theory anomaly free. It is highly believed that superpartners of the known particles should have masses below 1 TeV in order not to lose the good features of the SUSY. The direct experimental evidence for the sparticles is still lacking and the results of the experiments in the existing colliders indicate that squarks have masses $m_{\tilde{q}} \geq 130\text{GeV}$; consequently higher energy scale should be probed and it is desirable to reach the TeV scale at a constituent level [11,12]. Therefore it might be sensible to say that HERA, LEP, FERMILAB and LHC should be sufficient to check the idea of low energy SUSY, namely the scale between 100 GeV and 1 TeV, however experiments at all possible types of colliding beams would be inevitable to explore the new physics at the TeV scale.

In this report we will study the productions of SUSY particles in polarized TeV scale photon-proton collisions. Several SUSY production processes such as $\gamma p \rightarrow \tilde{q}\tilde{w}X$, $\gamma p \rightarrow \tilde{w}\tilde{w}X$, $\gamma p \rightarrow \tilde{q}\tilde{g}X$, $\gamma p \rightarrow \tilde{q}\tilde{\gamma}X$ (or $\tilde{q}\tilde{z}$) and $\gamma p \rightarrow \tilde{q}\tilde{q}^*X$ have already been discussed [6] without taking into account the initial beam polarizations. Polarization effects have been investigated in [9]. Also scalar leptoquark productions at TeV energy γp colliders have been investigated [7]. Let us first briefly review the polarization properties of high energy photon beams.

II. POLARIZED HIGH ENERGY GAMMA BEAMS

A beam of laser photons ($\omega_0 \approx 1.26\text{ eV}$, for example) with high intensity, about 10^{20} photons per pulse, is Compton-backscattered off high energy electrons ($E_e=250\text{ GeV}$, for example) from a linear accelerator and turns into hard photons with a conversion coefficient close to unity. The energy of the backscattered photons, E_γ , is restricted by the kinematic condition $y_{max} = 0.83$ (where $y = E_\gamma/E_e$) in order to get rid of background effects, in particular e^+e^- pair production in the collision of a laser photon with a backscattered photon in the conversion region.

The details of the Compton kinematics and calculations of the cross section can be found in ref. [1] (see Ginzburg et.al). The energy spectrum of the high energy real (backscattered) photons, $f_{\gamma/e}(y)$, is given by

$$f_{\gamma/e}(y) = \frac{1}{D(\kappa)} \left[1 - y + \frac{1}{1-y} - 4r(1-r) - \lambda_e \lambda_0 r \kappa (2r-1)(2-y) \right] \quad (1)$$

where $\kappa = 4E_e \omega_0 / m_e^2$ and $r = y/\kappa(1-y)$. Here λ_0 and λ_e are the laser photon and the electron helicities respectively, and $D(\kappa)$ is

$$D(\kappa) = \left(1 - \frac{4}{\kappa} - \frac{8}{\kappa^2} \right) \ln(1+\kappa) + \frac{1}{2} + \frac{8}{\kappa} - \frac{1}{2(1+\kappa)^2} \\ + \lambda_e \lambda_0 \left[\left(1 + \frac{2}{\kappa} \right) \ln(1+\kappa) - \frac{5}{2} + \frac{1}{1+\kappa} - \frac{1}{2(1+\kappa)^2} \right] \quad (2)$$

In our numerical calculations, we assume $E_e \omega_0 = 0.3 \text{ MeV}^2$ or equivalently $\kappa = 4.8$ which corresponds to the optimum value of $y_{max} = 0.83$, as mentioned above.

The energy spectrum, $f_{\gamma/e}(y)$, does essentially depend on the value $\lambda_e \lambda_0$. In the case of opposite helicities ($\lambda_e \lambda_0 = -1$) the spectrum has a very sharp peak at the high energy part of the photons. This allows us to get a highly monochromatic high energy gamma beam by eliminating low energy part of the spectrum [1] (see Ginzburg et.al and Borden et.al). On the contrary, for the same helicities ($\lambda_e \lambda_0 = +1$) the spectrum is flat.

The average degree of linear polarization of the photon is proportional to the degree of linear polarization of the laser. In our calculations, we assume that the degree of linear polarization of the laser is zero so that the final photons have only the degree of circular polarization ($\lambda(y) = \langle \xi_2 \rangle \neq 0$ and $\langle \xi_1 \rangle = \langle \xi_3 \rangle = 0$). The circular polarization of the backscattered photon is given as follows

$$\langle \xi_2 \rangle = \lambda(y) = \frac{(1-2r)\left(\frac{1}{1-y} + 1 - y\right)\lambda_0 + \lambda_e r \kappa \left(1 + (1-2r)^2(1-y)\right)}{\frac{1}{1-y} + 1 - y - 4r(1-r) - \lambda_0 \lambda_e r \kappa (2r-1)(2-y)} \quad (3)$$

For the same initial polarizations ($\lambda_0 \lambda_e = +1$), it is seen that $\lambda(y) \approx +1$, as nearly independent of y ; while for the case of the opposite polarizations ($\lambda_0 \lambda_e = -1$), the curve $\lambda(y)$ smoothly changes from -1 to $+1$ as y increases from zero to 0.83 [1].

III. PAIR PRODUCTION OF SQUARKS

We consider the minimal supersymmetric extension of the standard model (MSSM) which includes soft breaking terms. Here we have only taken into account the direct interaction of the photons with partons in the proton. The resolved contributions to the SUSY particle productions are relatively small, around 10% which do not affect our estimates for the discovery mass limits of new particles very much [13].

The invariant amplitude for the subprocess $\gamma g \rightarrow \tilde{q} \tilde{q}^*$ proceeds via the t-, u-channel squark exchange and four-point vertex interactions. The polarized differential cross-section of this subprocess can be calculated in terms of the usual Mandelstam variables $\hat{s} = (p_1 + p_2)^2$, $\hat{t} = (p_1 - p_3)^2$ and $\hat{u} = (p_1 - p_4)^2$ as :

$$\frac{d\hat{\sigma}}{d\hat{t}} = \left(\frac{d\hat{\sigma}}{d\hat{t}} \right)_{np} + \xi_2 \eta_2 \left(\frac{d\hat{\sigma}}{d\hat{t}} \right)_{pol} \quad (4)$$

$$\left(\frac{d\hat{\sigma}}{d\hat{t}} \right)_{np} = \frac{e^2 e_{\tilde{q}}^2 g_s^2}{8\pi \hat{s}^2} \left[1 + \frac{m_{\tilde{q}}^2 (3m_{\tilde{q}}^2 - \hat{s} - \hat{t})}{2(\hat{s} + \hat{t} - m_{\tilde{q}}^2)^2} + \frac{(3m_{\tilde{q}}^2 - \hat{s} + \hat{t})}{4(m_{\tilde{q}}^2 - \hat{t})} \right. \\ \left. + \frac{m_{\tilde{q}}^2 (m_{\tilde{q}}^2 + \hat{t})}{(m_{\tilde{q}}^2 - \hat{t})^2} + \frac{(5m_{\tilde{q}}^2 + 2\hat{s} - \hat{t})}{4(\hat{s} + \hat{t} - m_{\tilde{q}}^2)} + \frac{(\hat{s} - 2m_{\tilde{q}}^2)(\hat{s} - 4m_{\tilde{q}}^2)}{4(m_{\tilde{q}}^2 - \hat{t})(\hat{s} + \hat{t} - m_{\tilde{q}}^2)} \right] \quad (5)$$

$$\left(\frac{d\hat{\sigma}}{d\hat{t}} \right)_{pol} = \frac{e^2 e_{\tilde{q}}^2 g_s^2}{16\pi \hat{s}^2} \left[\frac{m_{\tilde{q}}^2 (\hat{s} - 2\hat{t}) + m_{\tilde{q}}^4 + \hat{s}\hat{t} + \hat{t}^2}{(m_{\tilde{q}}^2 - \hat{s} - \hat{t})(m_{\tilde{q}}^2 - \hat{t})} \right] \quad (6)$$

Here $e_{\tilde{q}}$ is the squark charge, $g_s = \sqrt{4\pi\alpha_s}$ is the strong coupling constant, $e = \sqrt{4\pi\alpha}$, α is the fine structure constant and ξ_2, η_2 are the circular polarization parameters of the photon and gluon respectively. After performing the integration over \hat{t} one can easily obtain the total cross section for the subprocess $\gamma g \rightarrow \tilde{q} \tilde{q}^*$ as follows :

$$\hat{\sigma}(\hat{s}, m_{\tilde{q}}, \xi_2, \eta_2) = \hat{\sigma}_{np} + \xi_2 \eta_2 \hat{\sigma}_{pol} \quad (7)$$

$$\hat{\sigma}_{np} = \frac{\pi \alpha e_{\tilde{q}}^2 \alpha_s}{2 \hat{s}} \left[2\beta(2 - \beta^2) - (1 - \beta^4) \ln \frac{1 + \beta}{1 - \beta} \right] \quad (8)$$

$$\hat{\sigma}_{pol} = \frac{\pi \alpha e_{\tilde{q}}^2 \alpha_s}{2 \hat{s}} \left[2\beta - 2(1 - \beta^2) \ln \frac{1 + \beta}{1 - \beta} \right] \quad (9)$$

where $\beta = (1 - 4m_{\tilde{q}}^2/\hat{s})^{1/2}$. The above expression in (4) is a cross section for left- squarks or right-squarks only, and a color factor of $C = 1/2$ is already included. In order to obtain the total cross section for the process $\gamma p \rightarrow \tilde{q}\tilde{q}^* X$ one should integrate $\hat{\sigma}$ over the gluon and photon distributions. For this purpose we make the following change of variables: first expressing \hat{s} as $\hat{s} = x_1 x_2 s$ where $\hat{s} = s_{\gamma g}$, $s = s_{ep}$, $x_1 = E_{\gamma}/E_e$, $x_2 = E_g/E_p$ and furthermore calling $\tau = x_1 x_2$, $x_2 = x$ then one obtains $dx_1 dx_2 = dx d\tau/x$. The limiting values are $x_{1,max} = 0.83$ in order to get rid of the background effects in the Compton backscattering, particularly e^+e^- pair production in the collision of the laser with the high energy photon in the conversion region, $x_{1,min} = 0$, $x_{2,max} = 1$, $x_{2,min} = \frac{\tau}{0.83}$, $\hat{s}_{min} = 4m_{\tilde{q}}^2$. Then we can write the total cross section with right circular polarized laser and spin-up proton beam polarized longitudinally as follows:

$$\begin{aligned} \sigma_{R\uparrow} = \int_{4m_{\tilde{q}}^2/s}^{0.83} d\tau \int_{\tau/0.83}^1 dx \frac{1}{x} \left\{ P \left[f_+^{\gamma}(\frac{\tau}{x}) f_{+\uparrow}^g(x) \hat{\sigma}(\tau s, m_{\tilde{q}}, 1, -1) + f_+^{\gamma}(\frac{\tau}{x}) f_{-\uparrow}^g(x) \hat{\sigma}(\tau s, m_{\tilde{q}}, 1, 1) \right] \right. \\ \left. + (1 - P) \left[f_+^{\gamma}(\frac{\tau}{x}) f_{+\downarrow}^g(x) \hat{\sigma}(\tau s, m_{\tilde{q}}, 1, 1) + f_+^{\gamma}(\frac{\tau}{x}) f_{-\downarrow}^g(x) \hat{\sigma}(\tau s, m_{\tilde{q}}, 1, -1) \right] \right\} \end{aligned} \quad (10)$$

where the $(\pm 1, \pm 1)$ inside $\hat{\sigma}$ refers to the values of the Stokes parameters (ξ_2, η_2) respectively. Using the Eq.(4) the above expression yields

$$\begin{aligned} \sigma_{R\uparrow} = \int_{4m_{\tilde{q}}^2/s}^{0.83} d\tau \int_{\tau/0.83}^1 dx \frac{1}{x} \left\{ P \left[f_+^{\gamma}(\frac{\tau}{x}) f_{unpol}^g(x) \hat{\sigma}_{np} + f_+^{\gamma}(\frac{\tau}{x}) (-\Delta f_{pol}^g(x)) \hat{\sigma}_{pol} \right] \right. \\ \left. + (1 - P) \left[f_+^{\gamma}(\frac{\tau}{x}) f_{unpol}^g(x) \hat{\sigma}_{np} + f_+^{\gamma}(\frac{\tau}{x}) (+\Delta f_{pol}^g(x)) \hat{\sigma}_{pol} \right] \right\} \end{aligned} \quad (11)$$

where P is the polarization percentage of spin-up protons in the beam and for a maximum attainable degree of 70% longitudinal polarization $P = 0.85$. Also f_{\pm}^{γ} and f_{\pm}^g are the polarized distributions for the photon and gluon inside the proton, respectively. In the numerical calculations we used the unpolarized and difference distributions, f_{unpol}^g and Δf_{pol}^g taken from [15]:

$$f_{unpol}^g(x) = \frac{1}{x} \left[(2.62 + 9.17x)(1 - x)^{5.90} \right] \quad (12)$$

and

$$\Delta f_{pol}^g = 16.3001 x^{-0.3} (1 - x)^7 \quad (13)$$

The energy spectrum of the high energy real photons $f_{\gamma}(y)$ is given as in Eq.(1-2). To carry out the numerical integration we take $e_{\tilde{q}} = 2/3$ hence consider only u-type squarks and $\alpha_s = 0.1$ is taken. The results of the numerical calculations clearly indicate that the process $\gamma p \rightarrow \tilde{q}\tilde{q}^* X$ has a detectable cross section. In Figs. V(a-c) the dependence on the squark masses is shown for different γp colliders. The relevant parameters of these machines are given in Table 1.

On the other hand observation limit for the new particles is taken to be 100 events per running year (10^7 seconds). This level of observability is considered to be satisfactory since the background is expected to be clearer than that encountered in the hadron colliders where 1000 events/year is usually desired due to the strong background processes. Hence taking into account the luminosity values given in Table I [see Aydin et al. in ref.1], one can easily find from the Figs. V(a-c) the upper mass limits for the squarks. These values of discovery limits are also tabulated in Table I. For the d-type squarks $(\tilde{d}_{L,R}, \tilde{s}_{L,R}, \tilde{b}_{L,R})$ putting $e_{\tilde{q}} = -1/3$, results in the decrease of the cross section by a factor $1/4$, but the corresponding upper mass values are approximately some seventy percent of those in the last column of the Table I. Furthermore the mixings among left and right squarks might be taken into consideration. Because their masses are expected to be close to each other, one can assume that \tilde{q}_L and \tilde{q}_R are degenerate in mass which points out that for the $\tilde{q}\tilde{q}^*$ production one can always consider the sum of the two cross section for \tilde{q}_L and \tilde{q}_R production.

Hence if we do this incoherent sum of \tilde{q}_L and \tilde{q}_R and with $m_{\tilde{q}_L} = m_{\tilde{q}_R}$ we must multiply the expression in (4) by an extra factor two, which increases the discovery limits for the squark masses. One additional assumption can be made by assuming five degenerate flavours of \tilde{q}_L and \tilde{q}_R , (namely except stop) which multiplies the individual squark pair production cross section, Eq.(3) by about a factor of six and a half. We see that the cross sections for different initial beam polarizations do not differ much which reflects the scalar nature of the squarks.

On the other hand the use of the polarized beams make it possible to look for the polarization asymmetries as a function of the squark masses. In Figs. V(a-c) we have presented the results of the polarization asymmetry using the results of the up and down polarized proton beams. Asymmetry has been defined through the following relation

$$A_{\uparrow\downarrow} = \frac{\sigma_{R\uparrow} - \sigma_{R\downarrow}}{\sigma_{R\uparrow} + \sigma_{R\downarrow}} \quad (14)$$

As can be seen from the Figures 2(a-c) the asymmetry is sensitive to the squark mass which can be useful for determination of the mass parameter. Furthermore another asymmetry might be defined considering the opposite polarizations of the laser beam. Hence left-right asymmetry defined with respect to the laser beam as

$$A_{LR} = \frac{\sigma_{R\uparrow} - \sigma_{L\uparrow}}{\sigma_{R\uparrow} + \sigma_{L\uparrow}} \quad (15)$$

The results of the calculations are plotted in Fig. V and a similar behaviour is seen.

Signature for the pair production of squarks: One characteristic feature of the R-parity conserving supersymmetric processes is the large missing energy. Usually photino mass is assumed to be less than $m_{\tilde{q}}$. This immediately implies that $\tilde{q} \rightarrow q\tilde{\gamma}$. The decay of the squark into photino is not the only possibility. For squark masses larger than 200-300 GeV and depending on the mass spectrum of the other SUSY particles there exist additional decay modes such as $\tilde{q} \rightarrow q\tilde{g}$, $\tilde{q} \rightarrow q\tilde{w}$, $\tilde{q} \rightarrow \tilde{q}W$, $\tilde{q} \rightarrow q\tilde{z}$. Branching ratios of these decays depend on the masses of these particles and coupling constants. One possibility of the decay of zino is the decay into a neutrino and a sneutrino. Both particles will not be observed like photinos. Therefore the signature for the process $\gamma p \rightarrow \tilde{q}\tilde{q}^* X$ will be in general multijets + lepton(s) + large missing energy and missing p_T . The definite polarization asymmetries associated with the missing energy and momentum may help in separating these events from the backgrounds.

Actually the production of the squark pairs in $ep \rightarrow \gamma^* g \rightarrow \tilde{q}\tilde{q}^*$ collisions via the quasi-real photon gluon fusion were studied before [13,14]. However in these studies Weizsacker-Williams approximation has been used for the quasi-real photon distribution $f_{\gamma/e}$. Since the WW-spectrum is much softer than the real γ spectrum the discovery mass limits for the squarks in our case turn out to be much higher than the conventional ep-colliders.

Finally our analysis shows that the future γp colliders can have considerable capacities in addition to the well known pp and e^+e^- colliders in the investigation of supersymmetric particles. We see that the range of squark masses that can be explored at various γp -machines (200 GeV - 0.85 TeV) are higher than the corresponding values at standard type ep -colliders (20 GeV - 80 GeV for HERA). Several LHC studies have shown that the reach for squarks will be greater than 1 TeV. But clearer backgrounds in a gamma-proton collider can be considered to be an advantageous feature in extracting supersymmetric signals.

IV. GLUINO-SQUARK PRODUCTION

In this section, the subprocess $\gamma q \rightarrow \tilde{q}\tilde{g}$ is considered taking into account the direct interaction of the photons with partons in the proton. The invariant amplitude for this subprocess is the sum of the terms corresponding to the s-channel quark exchange and u-channel squark exchange interactions. In order to take into consideration the polarization in the calculation of the differential cross-section we use the density matrices of the colliding beams. For polarized and unpolarized cases the density matrices of photon is given as follows:

$$\rho_{\mu\mu'}^{(\gamma)} = -\frac{1}{2}g_{\mu\mu'} \quad \text{unpolarized case} \quad (16)$$

$$\rho_{\mu\mu'}^{(\gamma)} = \frac{1}{2}(1 + \vec{\xi} \cdot \vec{\sigma})_{ab} e_{\mu}^{(a)} e_{\mu'}^{(b)} \quad \text{polarized case} \quad (17)$$

where $\vec{\sigma} = (\sigma_1, \sigma_2, \sigma_3)$ are the usual Pauli matrices and $\vec{\xi} = (\xi_1, \xi_2, \xi_3)$ are Stokes parameters of the backscattered laser photon. In our calculations we take into account only circular polarization which is determined by ξ_2 . For the right (left) circular polarization, ξ_2 takes the value of $+1(-1)$. $e_{\mu}^{(a)}$ ($a = 1, 2$) are the polarization unit 4-vectors which

are orthogonal to each other and to the momenta of the colliding particles. Density matrix for the quarks can be taken as in the form for the massless spin 1/2 particles since the mass of quark has been ignored in the calculation of the invariant amplitude.

$$\rho^q = \frac{1}{2} \gamma \cdot p (1 \pm 2\lambda_q \gamma^5) \quad (18)$$

Here λ_q refers to the helicities of the quarks inside the proton and takes the values of $+1/2(-1/2)$ for the positive (or negative) helicity corresponding to the spin direction to the parallel (or antiparallel) of its momentum. The calculation of differential cross-section has been performed in the center of mass frame. One can easily obtain the total cross-section $\hat{\sigma}$ for the subprocess under consideration by integrating over \hat{t} :

$$\hat{\sigma}(m_{\bar{g}}, m_{\bar{q}}, \hat{s}, \xi_2, \lambda_q) = C \frac{1}{2} (1 + 2\lambda_q) [A(m_{\bar{g}}, m_{\bar{q}}, \hat{s}) + \xi_2 B(m_{\bar{g}}, m_{\bar{q}}, \hat{s})] \quad (19)$$

here C is a coefficient which includes coupling constants and color factor, ξ_2 is the helicity for the backscattered laser photon. For the subprocess cross-section $\hat{\sigma}(m_{\bar{g}}, m_{\bar{q}}, \hat{s}, \xi_2, \lambda_q)$ we can use the following short notations:

$$\begin{aligned} \hat{\sigma}(\xi_2 = +1, \lambda_q = +\frac{1}{2}) &\equiv \hat{\sigma}_{++} \\ \hat{\sigma}(\xi_2 = -1, \lambda_q = +\frac{1}{2}) &\equiv \hat{\sigma}_{-+} \\ \hat{\sigma}(\xi_2 = +1, \lambda_q = -\frac{1}{2}) &\equiv \hat{\sigma}_{+-} = 0 \\ \hat{\sigma}(\xi_2 = -1, \lambda_q = -\frac{1}{2}) &\equiv \hat{\sigma}_{--} = 0 \end{aligned} \quad (20)$$

From Eq.(19) it can be easily seen that the last two relations in Eq.(20) vanish for $\lambda_q = -1/2$. In order to obtain the total cross-section for the process $\gamma p \rightarrow \bar{q} \bar{g} X$ one should perform the integration over the quark and photon distributions. After making the change of the variables as in the previous section (here $\tau_{\min} = (m_{\bar{g}} + m_{\bar{q}})^2/s$) one can write the total cross-section for the right circular polarized laser and spin-parallel proton beam polarized longitudinally as follows:

$$\begin{aligned} \sigma_{R\uparrow} = \int_{\tau_{\min}}^{0.83} d\tau \int_{\tau/0.83}^1 \frac{dx}{x} \left\{ P \left[f_+^\gamma\left(\frac{\tau}{x}\right) f_{+/\uparrow}^q(x) \hat{\sigma}_{++} + f_+^\gamma\left(\frac{\tau}{x}\right) f_{-/\uparrow}^q(x) \hat{\sigma}_{+-} \right] \right. \\ \left. + (1 - P) \left[f_+^\gamma\left(\frac{\tau}{x}\right) f_{+/\downarrow}^q(x) \hat{\sigma}_{+-} + f_+^\gamma\left(\frac{\tau}{x}\right) f_{-/\downarrow}^q(x) \hat{\sigma}_{++} \right] \right\} \end{aligned} \quad (21)$$

where P is the polarization percentage of spin-parallel protons in the beam and $f_\pm^\gamma(y)$ is the energy spectrum of the laser photons which is given as in Eqs.(1-2). In the numerical integration the helicity of the backscattered laser photon, λ_γ is taken as in Eq.(3).

The total cross-section expression in Eq.(21) can be rearranged by considering the distribution of the valance quark (u-type) inside the proton and written in the form of:

$$\sigma_{R\uparrow} = \int_{\tau_{\min}}^{0.83} d\tau \int_{\tau/0.83}^1 \frac{dx}{x} \left\{ f_+^\gamma\left(\frac{\tau}{x}\right) u_v^+(x) \hat{\sigma}_{++} \right\} \quad (22)$$

where u_v^+ , u-type valance quark distribution with the positive helicity, is defined by the sum of the nonpolarized and difference polarized quark distributions

$$u_v^+(x) = \frac{1}{2} (u_{np} + \Delta u_{pol}). \quad (23)$$

After inserting this expression into the Eq.(22) then we arrive at:

$$\sigma_{R\uparrow} = \int_{\tau_{\min}}^{0.83} d\tau \int_{\tau/0.83}^1 \frac{dx}{x} \left\{ f_+^\gamma\left(\frac{\tau}{x}\right) \frac{1}{2} (u_{np} + \Delta u_{pol}) \hat{\sigma}_{++} \right\}. \quad (24)$$

For the polarized and unpolarized valance quark distributions in the above expression, the following relations have been used [15].

$$u_{np}(x) = 2.751x^{-0.412}(1-x)^{2.69} \quad (25)$$

$$\Delta u_{pol}(x) = 2.139x^{-0.2}(1-x)^{2.4}. \quad (26)$$

After the numerical calculations we get the production cross sections for the gluino-squark process and show the dependence of the total cross sections on the masses of the SUSY particles for various proposed γp colliders in Figs.4(a-c) and Figs.5(a-c). The upper mass limits for SUSY particle can easily be found from the figures by using the luminosities given in Table 2. These values are calculated by taking 100 events per running year as the observation limit for SUSY particle and tabulated in the same table.

Furthermore it is possible to look at the polarization asymmetries as a function of the sparticle mass which can be useful for determination of the mass parameter. Asymmetry with respect to the polarization cases of the laser beam is defined as in Eq.(14). One can also consider another asymmetry defined using the results of the up and down polarized proton beams defined as before in Eq.(15). In Figs.6(a-c) we have presented the results of the polarization asymmetry with respect to the left-right polarized laser beams.

Signature for gluino-squark production: In order to maintain baryon and lepton number conservation one usually imposes R-parity in the SUSY models. If R-parity exactly conserved SUSY particles can only be produced in pairs and also processes give large missing energy. Usually the photino and sneutrino are taken as the lightest SUSY particles and will not be observed. The possible decay modes of squarks and gluinos depend on the mass spectrum and on the coupling constants. The gluino will decay into a squark and antiquark. The squark will mainly decay into a quark and a photino. There are also possible decays of the squark into a wino or a zino with the less branching ratios. One possibility of the decay of zino is the decay into a neutrino and a sneutrino. According to the results of decay channels, the signature for the process $\gamma p \rightarrow \tilde{q}\tilde{g}X$ might be in general multijets + large missing energy and missing p_T . The definite polarization asymmetries associated with the missing energy and momentum may help in separating these events from the backgrounds.

In conclusion, our analysis shows that the future γp colliders can have considerable capacities in addition to the well known pp and e^+e^- colliders in the investigation of supersymmetric particles.

V. SQUARK-CHARGINO PRODUCTION

The subprocess contributing to our physical process $\gamma p \rightarrow \tilde{w}\tilde{q}X$ is $\gamma q \rightarrow \tilde{w}\tilde{q}$. The invariant amplitude for the specific subprocess $\gamma u \rightarrow \tilde{w}^+\tilde{d}$ is the sum of the three terms corresponding to the s-channel u quark exchange, the t-channel \tilde{w} wino exchange and the u-channel \tilde{d} squark exchange interactions:

$$\begin{aligned} \mathcal{M}_a &= \frac{-iee_q g}{2\hat{s}} \bar{u}(p')(1 - \gamma_5)(\not{p} + \not{k}) \not{\epsilon} u(p) \\ \mathcal{M}_b &= \frac{-iege_{\tilde{w}}}{2(\hat{t} - m_{\tilde{w}}^2)} \bar{u}(p') \not{\epsilon}(\not{p} - \not{k} + m_{\tilde{w}})(1 - \gamma_5)u(p) \\ \mathcal{M}_c &= \frac{-iee_{\tilde{q}} g}{2(\hat{u} - m_{\tilde{q}}^2)} \bar{u}(p')(1 - \gamma_5)u(p)(p - p' + k') \cdot \epsilon \end{aligned} \quad (27)$$

where e_q , $e_{\tilde{q}}$ and $e_{\tilde{w}}$ are the quark, squark and wino charges, and $g = e/\sin\theta_w$ is the weak coupling constant. Note that we ignore the quark masses.

Since we are interested in the polarized cross-section, we use the following density matrices for the initial photon and quark:

$$\begin{aligned} \rho^{(\gamma)} &= \frac{1}{2}(1 + \vec{\xi} \cdot \vec{\sigma}) \\ \rho^{(q)} &= u\bar{u} = \not{p}[1 + \gamma_5(\lambda_q + \vec{\xi}_{\perp} \cdot \vec{\sigma}_{\perp})] \end{aligned} \quad (28)$$

where ξ_1 , ξ_2 and ξ_3 are Stokes parameters. We take into account only circular polarization for the photon which is defined by ξ_2 , as has been already mentioned in the previous section. λ_q stands for the helicity of the parton-quark that is $+1(-1)$ for the spin directions parallel (anti-parallel) to its momentum. The last term in the quark density matrix does not contribute, because after the integration over the azimuthal angle it vanishes.

One can easily obtain the differential cross section for the subprocess $\gamma u \rightarrow \tilde{w}^+\tilde{d}$ as follows

$$\frac{d\hat{\sigma}}{d\hat{t}} = \frac{\pi\alpha^2}{\hat{s}^2 \sin^2\theta_w} (1 + \lambda_q) \left[\frac{d\hat{\sigma}_0}{d\hat{t}} + \lambda(y) \frac{d\hat{\sigma}_1}{d\hat{t}} \right]. \quad (29)$$

Performing the $d\hat{t}$ integration from t_{min} to t^{max} which are given by

$$t_{min}^{max} = \frac{1}{2}(m_{\tilde{w}}^2 + m_{\tilde{q}}^2 - \hat{s}) \left[1 \mp \sqrt{1 - 4m_{\tilde{w}}^2 m_{\tilde{q}}^2 / (m_{\tilde{w}}^2 + m_{\tilde{q}}^2 - \hat{s})^2} \right] \quad (30)$$

we immediately get the total cross section as

$$\hat{\sigma}(m_{\tilde{w}}, m_{\tilde{q}}, \hat{s}, \lambda(y)) = \frac{\pi\alpha^2}{\hat{s}^2 \sin^2\theta_w} (1 + \lambda_q) \left[\hat{\sigma}_0(m_{\tilde{w}}, m_{\tilde{q}}, \hat{s}) + \lambda(y) \hat{\sigma}_1(m_{\tilde{w}}, m_{\tilde{q}}, \hat{s}) \right]. \quad (31)$$

Note that the cross sections (Eqs(29) and (31)) are zero for $\lambda_q = -1$ because of the fact that we ignore the quark mass. Integrating the subprocess cross-section $\hat{\sigma}$ over the quark and photon distributions we obtain the total cross-section for the physical process $\gamma p \rightarrow \tilde{w}\tilde{q}X$:

$$\sigma = \int_{(m_{\tilde{w}}+m_{\tilde{q}})^2/s}^{0.83} d\tau \int_{\tau/0.83}^1 \frac{dx}{x} f_{\gamma/e}(\tau/x) f_q(x) \hat{\sigma}(m_{\tilde{w}}, m_{\tilde{q}}, \hat{s}, \lambda(\tau/x)) \quad (32)$$

where the photon distribution function, $f_{\gamma/e}(y)$, is actually the normalized differential cross-section of the Compton backscattering, Eq.(1) ; $f_q(x)$ is the distribution of quarks inside the proton. We set $\lambda_q = +1$ and $f_q(x) \rightarrow u^+(x) = \frac{1}{2}(u_{unp} + \Delta u_{pol})$ for the u -type valence quark distribution. In our numerical calculations, we use the distribution functions given in Eqs.(25-26). Performing the integrations in Eq.(32) numerically we obtain the total cross-section for the associated wino-squark production. We plot the dependence of the total cross-sections on the masses of the SUSY particles for various proposed γp colliders in Figs. 7(a-c) for $\lambda_0\lambda_e = +1$ and -1 . By taking 100 events per running year as observation limit for a SUSY particle, one can easily find the upper discovery mass limits from these figures using the luminosities of the proposed γp colliders given in Table 3. These discovery limits are tabulated in the same table.

It may be more interesting to use a polarization asymmetry in determining the masses of SUSY particles. Such an asymmetry can be defined with respect to the product of the polarizations of the laser photon and the electron as follows

$$A = \frac{\sigma_- - \sigma_+}{\sigma_- + \sigma_+} \quad (33)$$

where σ_+ and σ_- are the polarized total cross-sections given in Figs. 7(a-c). The results of the polarization asymmetry are shown in Figs. 8(a-c) for three colliders. *Signature for the squark-chargino production:* If one compares the curves σ_+ and σ_- in Figs. 7(a-c) for each collider one sees that the polarized cross-sections for different polarization do not differ much from each other and also from the unpolarized ones. Therefore, the discovery mass limits for SUSY partners obtained with polarized beams are nearly equal to those obtained with unpolarized beams. But the polarization asymmetry is highly sensitive to the wino and the squark masses and as high as 0.4 for all cases. Especially in the case of $m_{\tilde{q}} = 250 \text{ GeV}$, the asymmetry parameter A is around 0.6 for the higher wino masses.

The signature of the associated $\tilde{w}^+ \tilde{d}$ production will depend on the mass spectrum of SUSY particles. It is generally assumed that the photino and sneutrino are the lightest SUSY particles and that the hierarchy of the squark masses is similar to that of quarks. With these assumption we have the following decays for the case $m_{\tilde{q}} = m_{\tilde{w}}$:

$$\tilde{d} \rightarrow d\tilde{\gamma}, d\tilde{q} \text{ and } \tilde{w} \rightarrow l^+\tilde{\nu}, \nu\tilde{l}^+, W^+\tilde{\gamma}$$

By taking into account the further decays $\tilde{l}^+ \rightarrow l\tilde{\gamma}$ and $W^+ \rightarrow l^+\nu, q\bar{q}$ we arrive at the ultimate final states as $l^+ + n \text{ jets}(n = 1, 3, 5) + \text{large missing energy and missing } P_T$

The main background for the final state $l^+ + jet + P_T^{miss}$ will come from the process $\gamma q \rightarrow Wq \rightarrow l^+\nu q$; but this background may be reduced, in principle, by the cut $P_T^{miss} > 45 \text{ GeV}$ if $m_{\tilde{w}} \gg m_W$.

- [1] R.N.Milburn, Phys.Rev.Lett.**10**(1963)75
I.F.Ginzburg et al.,Nucl.Instrum. and Meth.**205**(1983)47
I.F.Ginzburg et al.,Nucl.Instrum. and Meth.**219**(1984)5
V.I.Telnov, Nucl.Instrum.and Meth.**A294**(1990)72
D.L.Borden,D.A.Bauer and D.O.Caldwell, SLAC preprint SLAC-5715 Stanford (1992)
Z.Z.Aydin, A.K.Çiftçi and S.Sultansoy, Nucl.Instrum.and Meth.**A351**(1994)261.

- [2] S.I.Alekhin et al., IHEP preprint 87-48 (1987)
 Z.Z.Aydin, A.K.Çiftçi and S.Sultansoy, *ibid*
 Z.Z.Aydin, A.K.Çiftçi and S.Sultansoy, Turkish J.Phys.**19**(1995)773
 P.Grosse-Wiesmann, Nucl.Instrum. and Meth.**A274**(1989)21
 M.Tigner, B.Wiik and F.Willeke, Proc.Part.Acc.Conf. San Fransisco (1991) v.5,p.2910
- [3] J.A.Grifols and R.Pascual, Phys.Lett.**B135**(1984)319
 E.Boos et al., Phys.Lett.**B173**(1991)273
 E.Boos et al., DESY preprint 91-114 Hamburg(1991)
 J.E.Cieza Montalvo and O.J.P.Eboli, Phys.Rev.**D47**(1993)837
 M.Nadeau and D.London,Phys.Rev.**D47**(1993)3742.
- [4] A.Goto and T.Kon, Europhys.Lett.**13**(1990)211
 T.Kon and A.Goto, Phys.Lett.**B295**(1992)324
 F.Cuyppers et al.,Nucl.Phys.**B383**(1992)45
 A.Goto and T.Kon, Europhys.Lett.**19**(1992)575
 H.Konig and K.A.Peterson, Phys.Lett.**B294**(1992)110
 F.Cuyppers et al.,Nucl.Phys.**B409**(1993)144
 T.Kon,Proc.of Fourth Workshop of JLC,KEK p.47 (1993).
- [5] S.I.Alekhin et al.,Int.J.of Mod.Phys. **A6**,(1991)23
 E.Boos et al., Proc. 26th Moriond Conf.p.501 (1991)Moriond, France
 G.Jikia,Nucl.Phys.**B333**,(1990)317.
- [6] W.Büchmüller and Z.Fodor, Phys.Lett.**B316**,(1993)510.
 A.T.Alan, Z.Z.Aydin and S.Sultansoy, Phys.Lett.**B327**(1994)70.
 A.T.Alan, S.Atağ, and Z.Aydin, J.Phys.G.**20**(1994)1399
- [7] S.Atağ, A.Çelikel and S.Sultansoy , Phys.Lett.**B326**,(1994)185.
 S.Atağ and O.Çakır, Phys.Rev.**D49**,(1994)5769.
 O.Çakır and S.Atağ, J.Phys.G.**21**(1995)1189
- [8] Z.Z.Aydin et al.,Int.J.Mod.Phys.A **11**(1996)2019
- [9] A.Kandemir and A.U.Yilmazer,Phys.Lett.B,**208**(1998)175
 A.Kandemir and A.U.Yilmazer,Nuovo Cim.A,**112**(1999)597
 Z.Aydin and O.Yilmaz, Europhys.Lett.**50**(2000)22
- [10] H.E.Haber and G.L.Kane,Phys.Rep.**C117**,(1986)75
 H.P.Nilles, Phys.Rep.**C110**,(1984)1
- [11] Perspectives on Supersymmetry, ed.by G.L.Kane, World-Scientific (1998)
- [12] H.Baer et al. CERN-PPE/95-45 (1995).
- [13] M.Drees and K.Grassie,Z.Phys.**C28**,(1985)451.
- [14] K.J.F.Gaemers and M.J.F.Janssen,Z.Phys.**C48**,(1990)491.
- [15] E.Eichten et al.,Rev.of Mod.Phys.**56**,(1984)579
 A.D.Martin and W.J.Stirling, Phys.Rev.**D50**(1994)6734

(a-c) Production cross sections of squark pairs as a function of their masses for various γp colliders. In each figure the polarization states of the beams are indicated as follows: Line: Unpolarized beams, linespoints: right polarized laser, up protons, dots: right polarized laser, down protons

(a-c) Up-down asymmetry versus squark masses for different γp colliders.

Left-right asymmetry versus squark mass for the HERA+LC γp collider.

(a-c) Production cross sections for gluino-squark as a function of their masses for various colliders. Each figure corresponds to right circular polarized laser and spin-parallel proton beam polarized longitudinally.

(a-c) Production cross sections for gluino and squarks as a function of their masses for various colliders. Each figure corresponds to left circular polarized laser and spin-parallel proton beam polarized longitudinally.

(a-c) Left-right polarization asymmetries versus sparticle masses for different γp colliders.

(a-c) Squark-wino production cross-sections as a function of the mass. Two thin curves on the left stand for the collider HERA+LC, middle curves for LHC+Linac 1 and two curves on the right for LHC+TESLA. A little bit higher (lower) curve of each twin is for $\lambda_0\lambda_e = -1$ ($\lambda_0\lambda_e = +1$), i.e., σ_- (σ_+).

(a-c) Polarization asymmetries as a function of the mass. Thin curve stands for the collider HERA+LC, middle curve for LHC+Linac 1 and thick curve for LHC+TESLA.

TABLE I. Parameters of γp colliders and discovery limits for scalar quarks with $e_{\tilde{q}} = 2/3$. (Note: $\sqrt{s_{\gamma p}}^{max} = 0.91\sqrt{s_{ep}}$)

| Machines | $\sqrt{s_{ep}}$ (TeV) | $\mathcal{L}_{\gamma p}$ ($10^{30} cm^{-2} s^{-1}$) | $m_{\tilde{q}}$ (TeV) (non-degenerate) squarks | $m_{\tilde{q}}$ (TeV) (degenerate) squarks |
|-------------|--------------------------|--|--|--|
| HERA+LC | 1.28 | 25 | 0.2 | 0.3 |
| LHC+TESLA | 5.55 | 500 | 0.85 | 1.1 |
| LHC+e-Linac | 3.04 | 500 | 0.6 | 0.7 |

TABLE II. Parameters of different γp colliders and discovery mass limits for scalar quarks and gluinos. (Note: $\sqrt{s_{\gamma p}}^{max} = 0.91\sqrt{s_{ep}}$)

| Machines | $\sqrt{s_{ep}}$ (TeV) | $\mathcal{L}_{\gamma p}$ ($10^{30} cm^{-2} s^{-1}$) | $m_{\tilde{u}} = m_{\tilde{g}}$ (TeV) | $m_{\tilde{u}} = 0.10$ $m_{\tilde{g}}$ (TeV) | $m_{\tilde{g}} = 0.10$ $m_{\tilde{u}}$ (TeV) |
|-------------|--------------------------|--|--|---|---|
| HERA+LC | 1.28 | 25 | 0.17 | 0.32 | 0.21 |
| LHC+TESLA | 5.55 | 500 | 0.77 | 1.90 | 1.05 |
| LHC+e-Linac | 3.04 | 500 | 0.53 | 1.22 | 0.75 |

TABLE III. Energy and luminosity values of different γp colliders. The discovery mass limits for squarks and winos are given in last three columns for $\lambda_0\lambda_e = +1$ ($\lambda_0\lambda_e = -1$).

| Machines | $\sqrt{s_{ep}}$ (TeV) | $\mathcal{L}_{\gamma p}$ ($10^{30} cm^{-2} s^{-1}$) | $m_{\tilde{q}} = m_{\tilde{w}}$ (TeV) | $m_{\tilde{q}} = 0.25$ $m_{\tilde{w}}$ (TeV) | $m_{\tilde{w}} = 0.10$ $m_{\tilde{q}}$ (TeV) |
|-------------|--------------------------|--|--|---|---|
| HERA+LC | 1.28 | 25 | 0.23(0.25) | 0.18(0.23) | 0.35(0.40) |
| LHC+Linac 1 | 3.04 | 500 | 0.65(0.70) | 1.00(1.15) | 1.33(1.48) |
| LHC+TESLA | 5.55 | 500 | 0.95(1.05) | 1.55(1.70) | 2.15(2.50) |

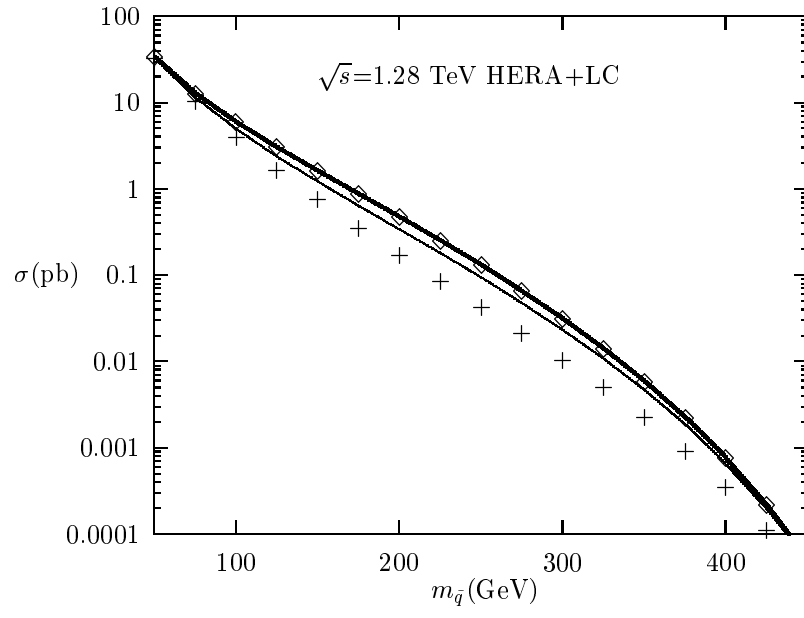


Fig.1.a

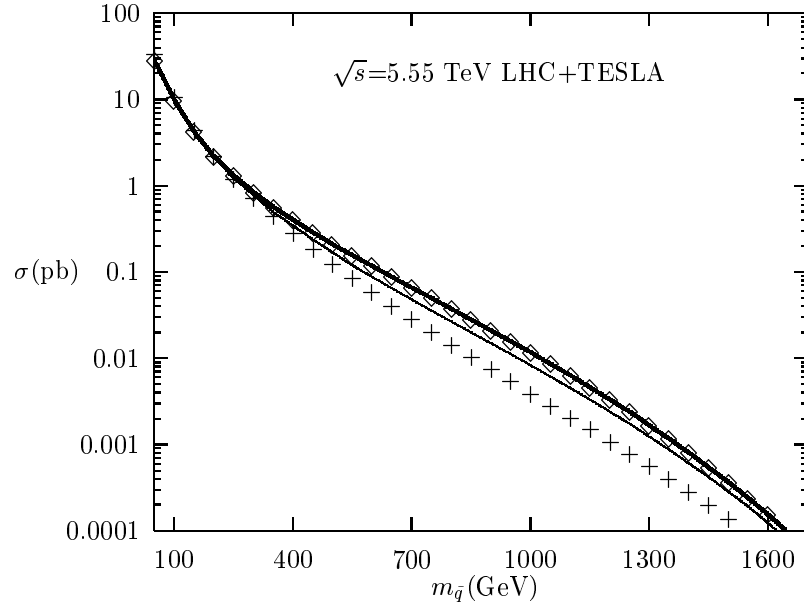


Fig.1.b

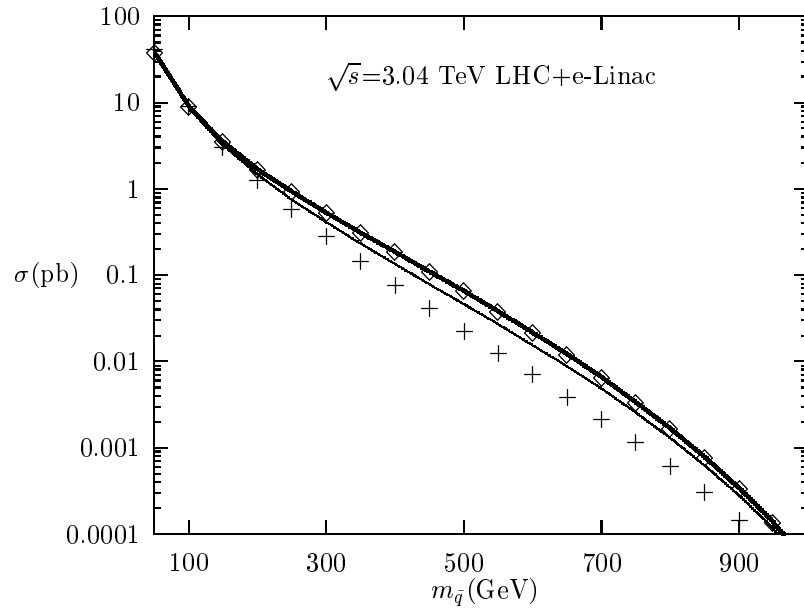


Fig.1.c

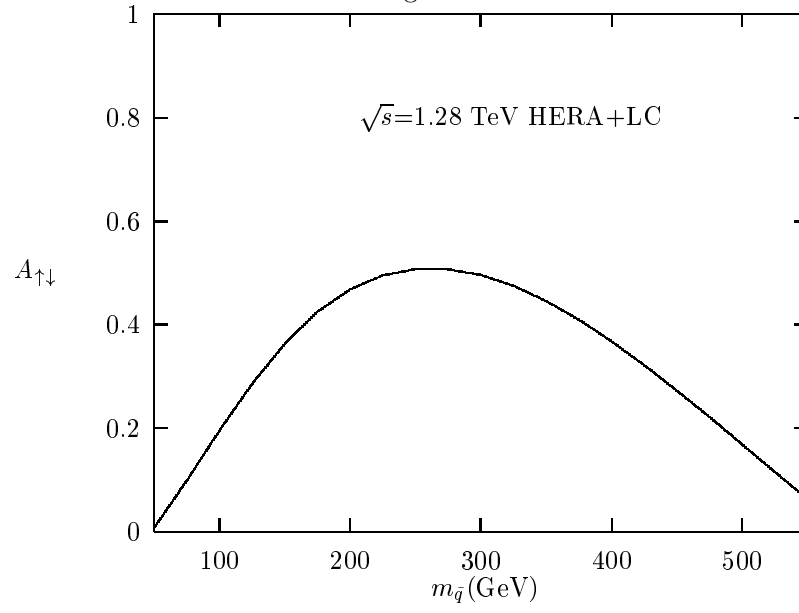


Fig.2.a

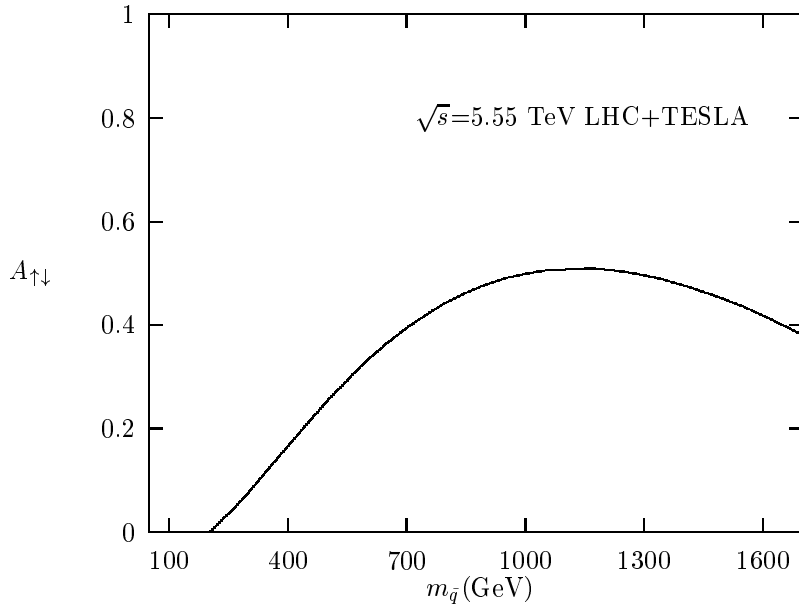


Fig.2.b

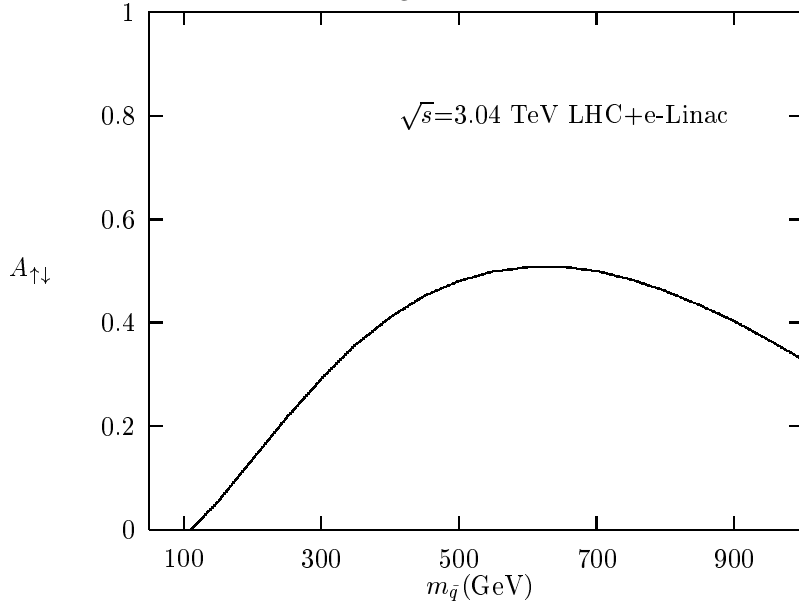


Fig.2.c

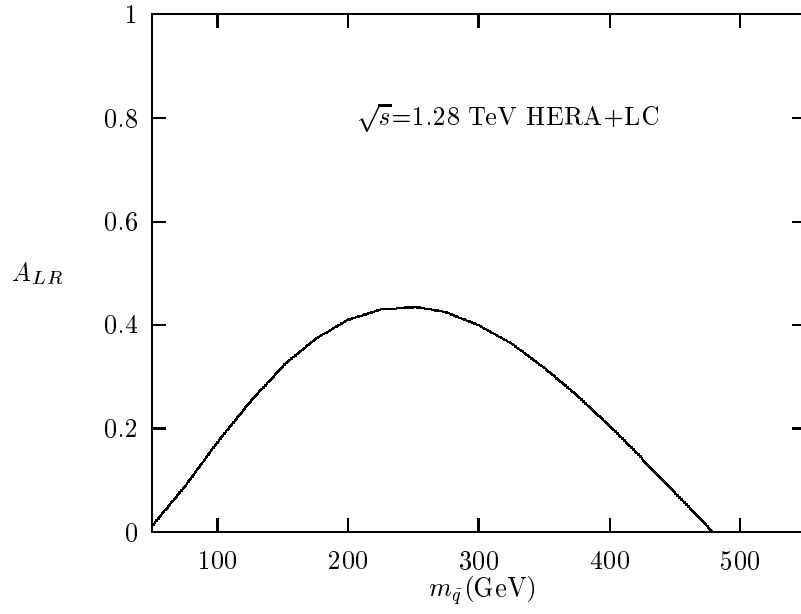


Fig.3.b

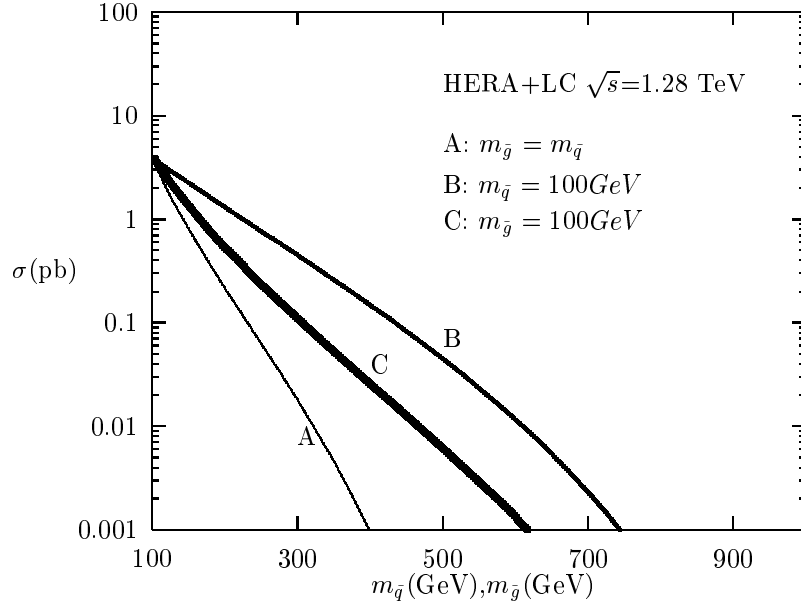


Fig.4.a

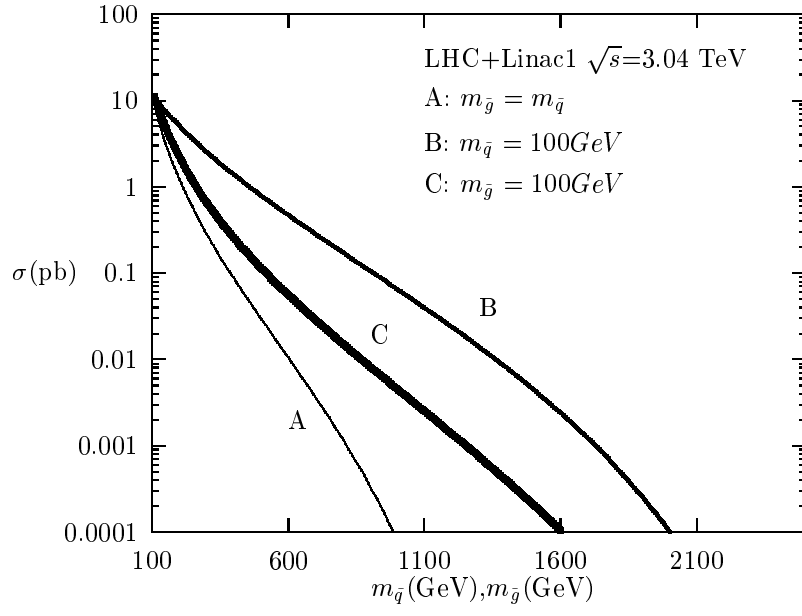


Fig.4.b

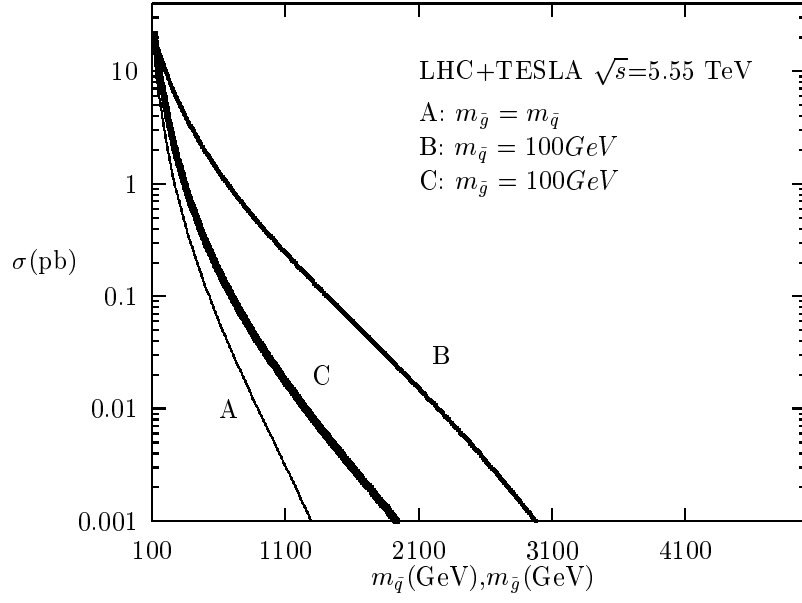


Fig.4.c

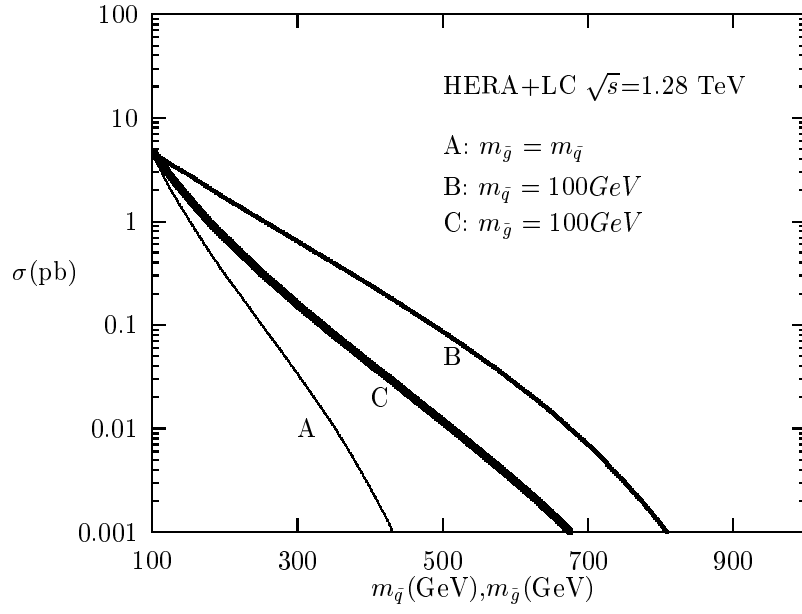


Fig.5.a

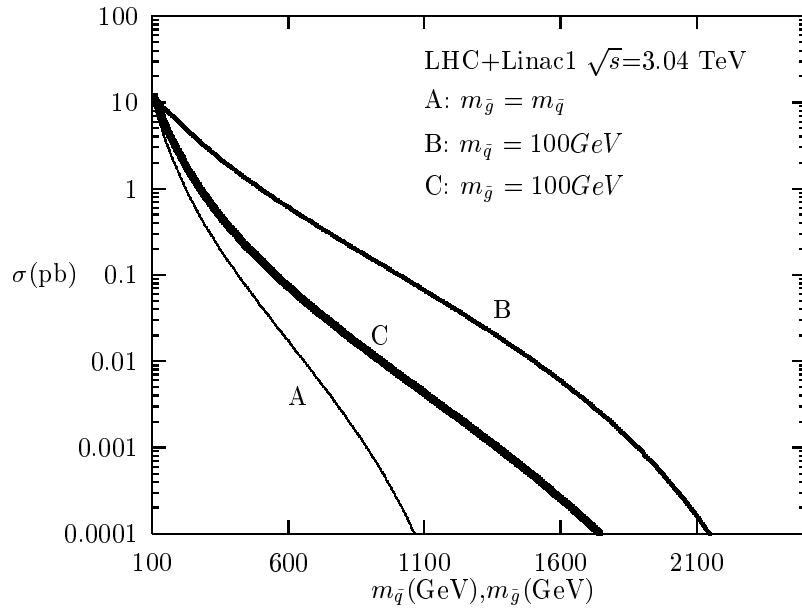


Fig.5.b

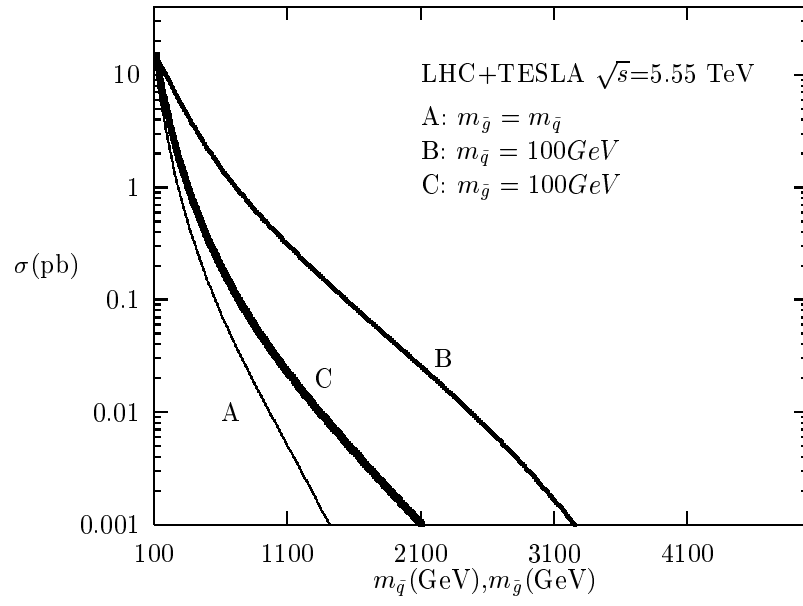


Fig.5.c

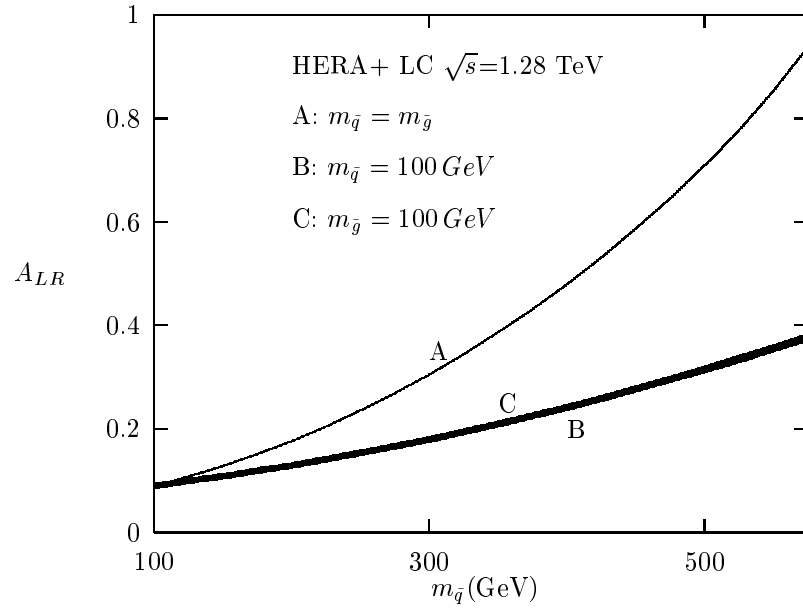


Fig.6.a

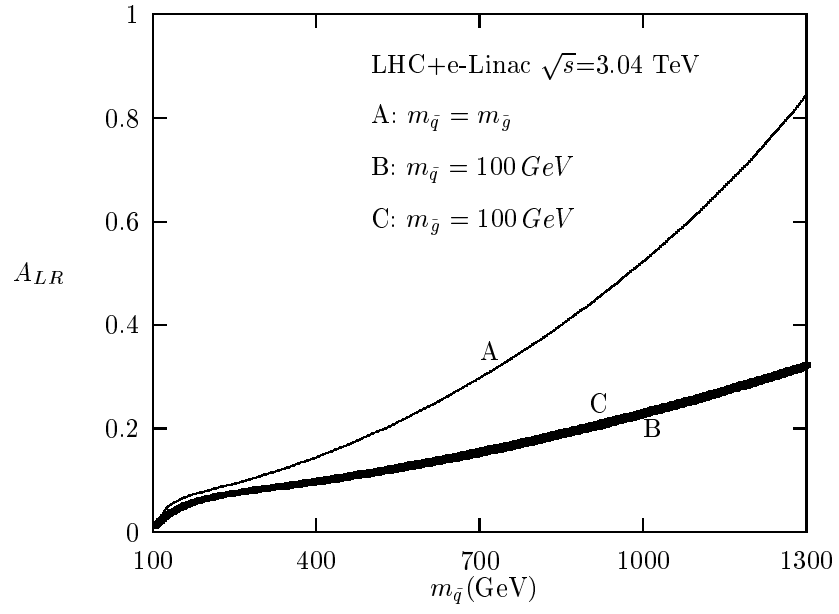


Fig.6.b

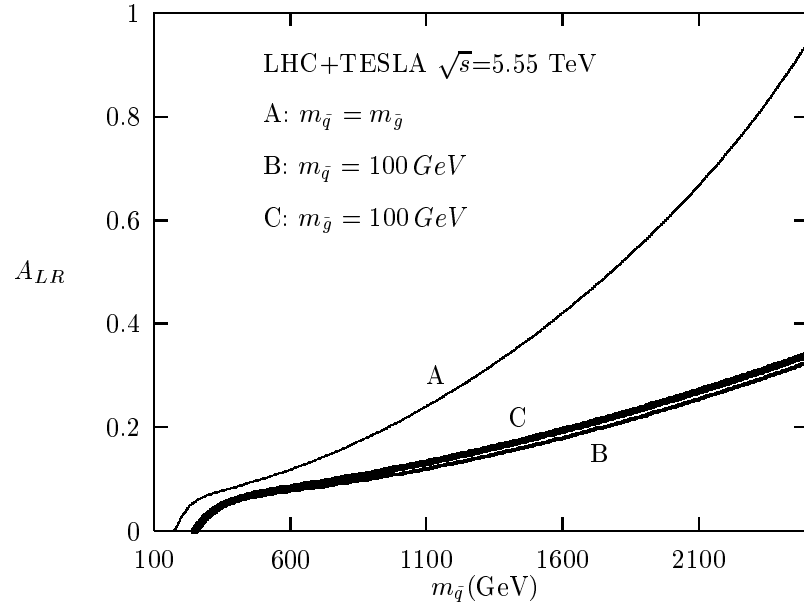


Fig.6.c

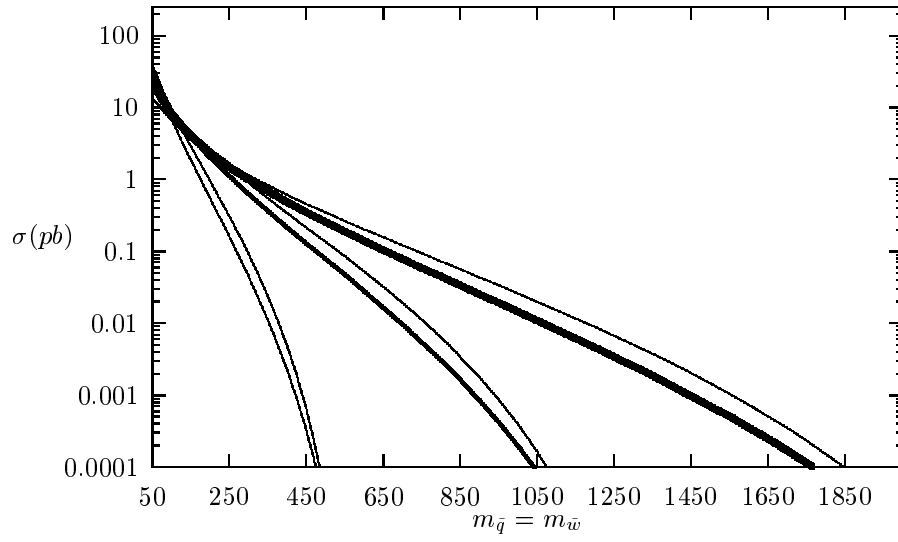


Fig.7.a

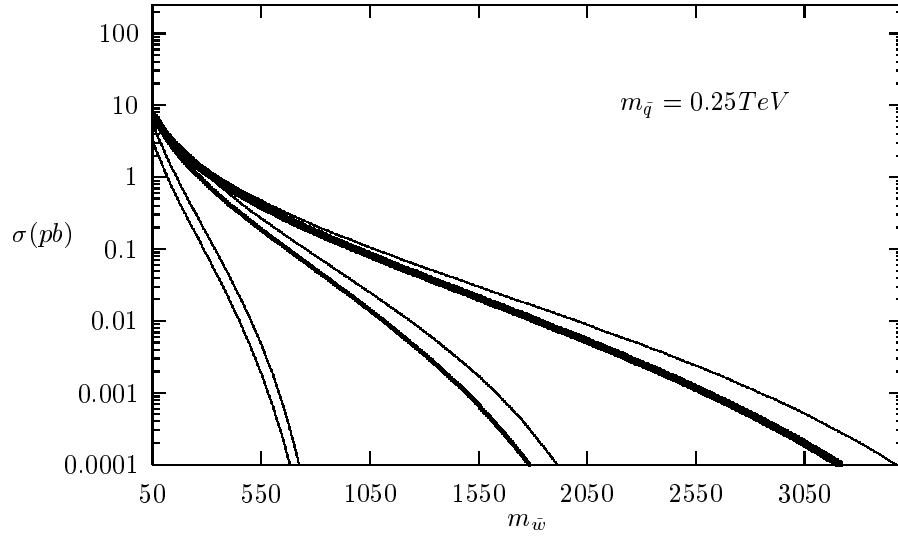


Fig.7.b

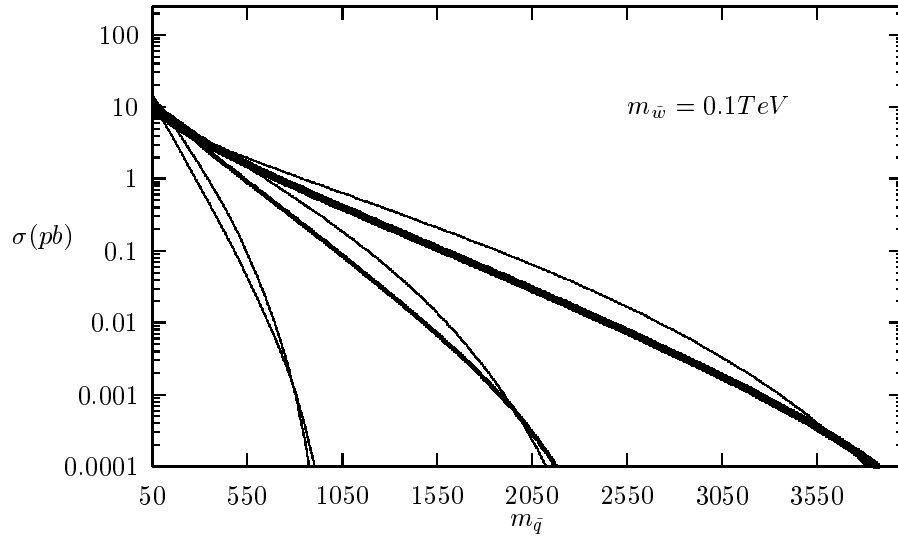


Fig.7.c

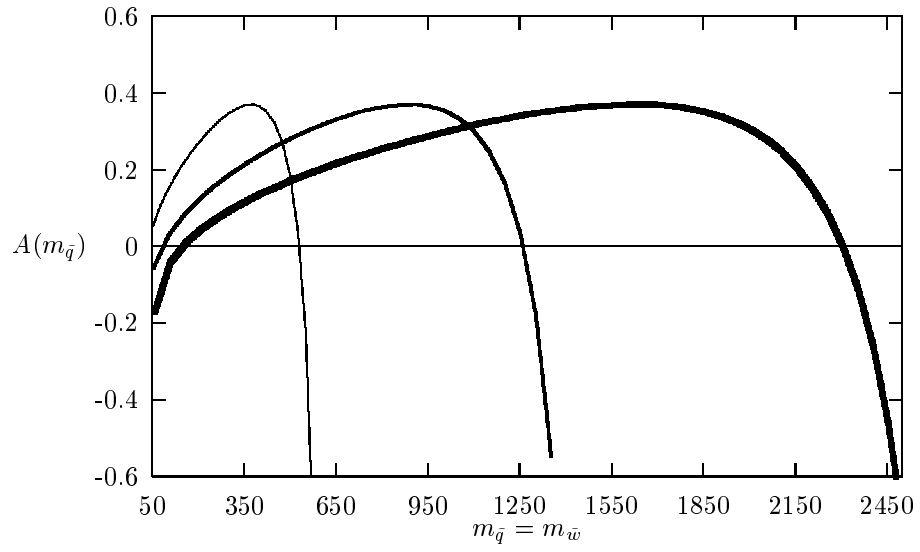


Fig.8.a

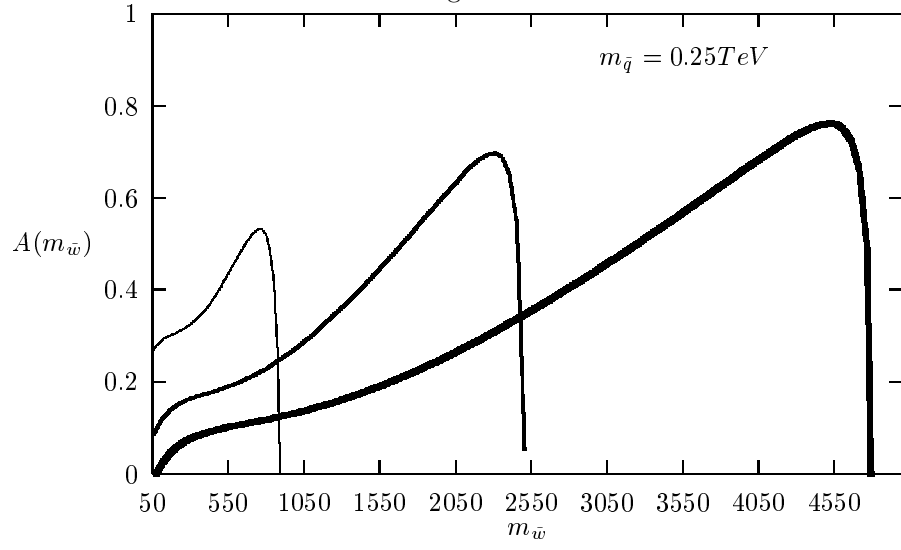


Fig.8.b

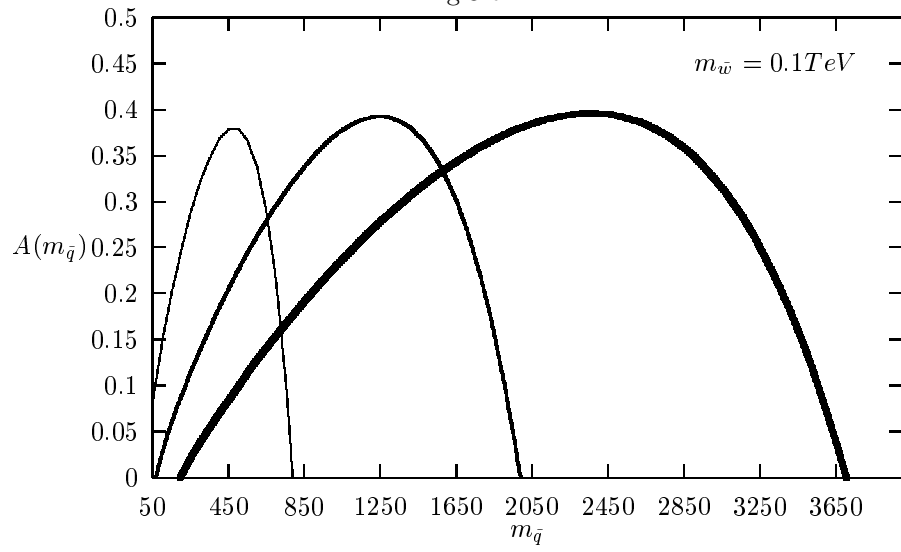


Fig.8.c